Reactions of Cerium Atoms and Dicerium Molecules with CO: Formation of Cerium Carbonyls and Photoconversion to CO-Activated Insertion Molecules

Mingfei Zhou,*,† Xi Jin,† and Jun Li*,‡

Department of Chemistry & Laser Chemistry Institute, Shanghai Key Laboratory of Molecular Catalysts and Innovative Materials, Fudan University, Shanghai 200433, China, and Department of Chemistry & Key Laboratory of Organic Optoelectronics and Molecular Engineering of Ministry of Education, Tsinghua University, Beijing 100084, China

Received: April 3, 2006; In Final Form: June 21, 2006

Reactions of cerium with carbon monoxide molecules in solid argon have been studied using matrix isolation infrared absorption spectroscopy. The cerium carbonyls CeCO and Ce_2CO are produced spontaneously on annealing and they are photochemically rearranged to the CCeO and *c*-$Ce_2(\mu$-C)(μ-O) isomers, where Ce and Ce_2 are inserted into the CO triple bond. Theoretical calculations indicate that CeCO is an end-on-bonded carbonyl with a quintet ground state, whereas Ce_2CO is a rare dinuclear lanthanide carbonyl complex with CO serving as an asymmetrically bridged, side-on ligand. The CCeO molecule was theoretically characterized to have a linear structure with a singlet ground state. Evidence is also presented for the $CeCO^-$ anion and other cerium carbonyls with higher coordination numbers.

Introduction

Carbon monoxide activation and reduction are important in numerous industrial processes such as hydroformylation, alcohol synthesis, and acetic acid synthesis.[1] The reactions of carbon monoxide with transition-metal and main-group element atoms and clusters have been extensively studied. A variety of transition-metal and main-group metal carbonyl complexes have been experimentally characterized, and theoretical studies of the electronic structures and bonding of these complexes have been carried out.[2−6]

The spectra, structures, and bonding of f-element metal carbonyls have also gained considerable attention. Binary f-element metal carbonyls were prepared in noble gas matrixes by co-deposition of thermally evaporated metal atoms with CO and noble gases at cryogenic temperatures and were spectroscopically characterized by several groups.[7−11] Some stable organouranium carbonyl complexes have also been synthesized.[12] Recent infrared spectroscopic investigations of the reactions of laser-ablated actinide metal atoms (Th and U) with CO have demonstrated remarkable CO activation via actinide metal carbonyl complexes. The monocarbonyls MCO (M = Th and U) can be isomerized to the inserted carbide−oxide molecules CMO, and the dicarbonyls undergo photoinduced rearrangement to the OMCCO and OTh(η^3-CCO) or (η^2-C_2)-UO_2 isomers.[13,14]

Here we report a combined matrix-isolation infrared spectroscopic and theoretical study of the reactions of cerium atoms and dicerium molecules with carbon monoxide. We will show that the end-on-bonded CeCO monocarbonyl and a unique side-on-bonded $Ce_2[\eta^2(\mu$-C,O)] dinuclear carbonyl are formed on annealing, and they undergo photoinduced rearrangement to the inserted products CCeO and a cyclic *c*-$Ce_2(\mu$-C)(μ-O) molecule.

* Corresponding author. E-mail: mfzhou@fudan.edu.cn (M.Z.), junli@tsinghua.edu.cn (J.L.)

† Fudan University.

‡ Tsinghua University.

Experimental and Computational Methods

The experiment for laser ablation and matrix isolation infrared spectroscopy is similar to those used previously.[15] Briefly, a Nd:YAG laser fundamental (1064 nm, 10 Hz repetition rate with 10 ns pulse width) was focused onto the rotating cerium metal target. The laser-ablated cerium atoms were co-deposited with CO in excess argon onto a CsI window cooled normally to 6 K by means of a closed-cycle helium refrigerator (ARS, 202N). The matrix gas deposition rate was typically 4 mmol/h. Carbon monoxide (Shanghai BOC, 99.99%), $^{13}C^{16}O$ (99%, Cambridge Isotopic Laboratory), and $^{12}C^{18}O$ (95%, Isotec) were used to prepare the CO/Ar mixtures. In general, matrix samples were deposited for 1−2 h. After sample deposition, IR spectra were recorded on a Bruker IFS66V spectrometer at 0.5 cm^{-1} resolution using a liquid nitrogen cooled HgCdTe (MCT) detector for the spectral range of 4000−400 cm^{-1}. Samples were annealed at different temperatures and subjected to broad-band irradiation using a high-pressure mercury arc lamp with glass filters.

Quantum chemical calculations were performed to determine the molecular structures and to help the assignments of vibrational frequencies of the observed reaction products. The calculations were performed at the level of density functional theory (DFT) with the B3LYP method, where the Becke three-parameter hybrid functional and the Lee−Yang−Parr correlation functional were used.[16] The 6-311+G(d) basis sets were used for the C and O atoms, and the scalar-relativistic SDD pseudopotential and (12s,11p,9d,8f)/[5s,5p,4d,3f] basis set were used for the Ce atom (basis-I).[17,18] Geometries were fully optimized and vibrational frequencies were calculated with analytical second derivatives. These DFT calculations were performed using the Gaussian 03 program.[19] Because of the complexity of the cerium carbide−oxide complex, we also carried out further calculations on the different states of CCeO at the coupled cluster level with single and double excitations plus perturbative triple excitations (CCSD(T)). These calculations used the same SDD pseudopotential for Ce, with a newly

10.1021/jp062073w CCC: $33.50
Published on Web 08/09/2006

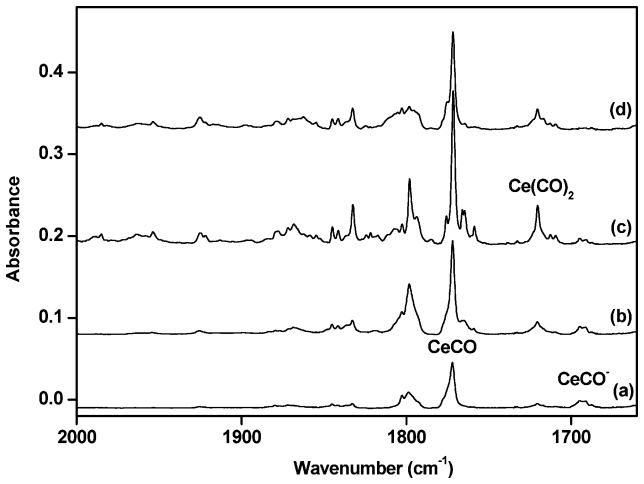

Figure 1. Infrared spectra in the 2000−1660 cm^{-1} region from co-deposition of laser-ablated cerium atoms with 0.1% CO in argon: (a) 1 h of sample deposition at 6 K, (b) after annealing to 25 K, (c) after annealing to 30 K, and (d) after 20 min $300 < \lambda < 580$ nm irradiation.

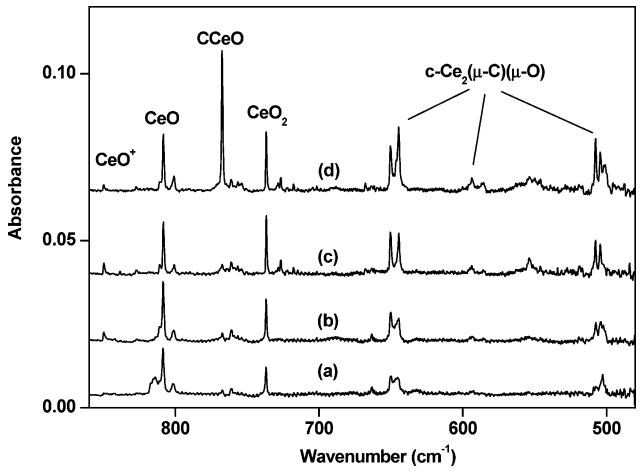

Figure 2. Infrared spectra in the 860−480 cm^{-1} region from co-deposition of laser ablated cerium atoms with 0.1% CO in argon: (a) 1 h of sample deposition at 6 K, (b) after annealing to 25 K, (c) after annealing to 30 K, and (d) after 20 min $300 < \lambda < 580$ nm irradiation.

developed (14s,13p,10d,8f,6g)/[6s,6p,5d,4f,3g] ANO basis sets for Ce[20] and cc-pVQZ basis sets for C and O (basis-II).[21,22] These large basis sets are necessary for correctly predicting the relative energies of CCeO, but they are too large for frequency calculations. The CCSD(T) frequency calculations were performed with geometries re-optimized using the third basis set (basis-III), where the same SDD basis sets and pseudopotential as basis-I were used for Ce, with the cc-pVDZ basis sets for C and O.[21,22] These CCSD(T) calculations were performed using MOLPRO 2002.[23]

Results and Discussion

Infrared Spectra. A series of experiments has been done using different CO concentrations (ranging from 0.025% to 0.2% in argon) and different laser energies to control the relative concentrations of Ce and CO. The infrared spectra in selected regions with 0.1% CO in argon using relatively high laser energy are illustrated in Figures 1 and 2, respectively, and the band positions are listed in Table 1. In the terminal C−O stretching frequency region (Figure 1), absorptions at 1771.8 and 1694.7 cm^{-1} were observed on sample deposition. The 1694.7 cm^{-1} band remained almost unchanged on sample annealing, but it

TABLE 1: Infrared Absorptions (cm^{-1}) from Co-Deposition of Laser-Ablated Cerium Atoms with CO in Excess Argon

$^{12}C^{16}O$	$^{13}C^{16}O$	$^{12}C^{18}O$	assignment[a]
1771.8	1733.0	1730.3	CeCO
1798.0	1759.1	1755.9	CeCO site
1694.7	1657.5	1655.5	$CeCO^-$
767.4	764.8	737.2	CCeO
646.4		639.8	CCeO
1142.7	1117.7	1122.5	$Ce_2[\eta^2(\mu\text{-C,O})]$
644.5	626.3	638.6	$c\text{-}Ce_2(\mu\text{-C})(\mu\text{-O})$
650.4	631.5	644.8	site
593.8			$c\text{-}Ce_2(\mu\text{-C})(\mu\text{-O})$
507.6	504.0	484.6	$c\text{-}Ce_2(\mu\text{-C})(\mu\text{-O})$
504.3	500.9	481.4	site
1720.3	1683.9	1678.8	$Ce(CO)_2$
1832.5	1792.2	1790.1	$Ce(CO)_x$
1845.0	1803.8	1802.6	$Ce(CO)_x$
1925.2	1882.5	1880.5	$Ce(CO)_x$
1953.7	1912.5	1906.1	$Ce(CO)_x$
1985.1	1942.2	1936.6	$Ce(CO)_x$
1403.6	1372.4	1372.9	$Ce_x(CO)_y$
1386.4	1355.6	1355.7	$Ce_x(CO)_y$

[a] "site" means the same molecule is trapped in a different matrix site. *x* and *y* are undetermined numbers of atoms.

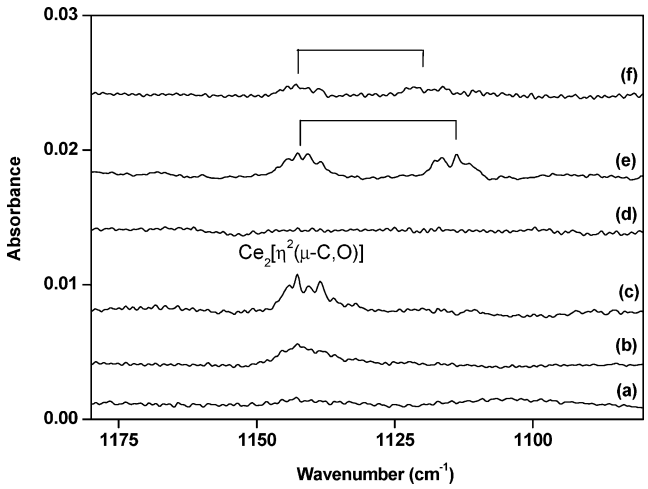

Figure 3. Infrared spectra in the 1180−1080 cm^{-1} region from co-deposition of laser-ablated cerium atoms with CO in excess argon: (a) 0.1% $^{12}C^{16}O$, 1 h of sample deposition, (b) after annealing to 25 K, (c) after annealing to 30 K, (d) after 20 min of $300 < \lambda < 580$ nm irradiation, (e) 0.05% $^{12}C^{16}O$ + 0.05% $^{13}C^{16}O$, after 30 K annealing, and (f) 0.05% $^{12}C^{16}O$ + 0.05% $^{12}C^{18}O$, after 30 K annealing.

disappeared upon broad-band ($300 < \lambda < 580$ nm) irradiation. The 1771.8 cm^{-1} band readily increased on annealing and decreased upon $300 < \lambda < 580$ nm irradiation. Several absorptions at 1720.3, 1832.5, 1845.0, 1925.2, and 1953.7 cm^{-1} were produced on sample annealing. These absorptions increased on higher temperature annealing and decreased upon $300 < \lambda < 580$ nm irradiation. Very weak absorptions at 1142.7 cm^{-1} appeared on sample annealing and were destroyed upon $300 < \lambda < 580$ nm irradiation (Figure 3). In the low-frequency region (Figure 2), absorptions due to CeO^+ (849.7 cm^{-1}), CeO (808.4 cm^{-1}), and CeO_2 (736.8 cm^{-1}) were observed.[24] In addition, two doublets at 650.4/644.5 and 507.6/504.3 cm^{-1} were observed on sample deposition, sharpened on annealing, and increased when the sample was subjected to $300 < \lambda < 580$ nm irradiation. A sharp new band at 767.4 cm^{-1} was produced under $300 < \lambda < 580$ nm irradiation.

Different isotopic labeled carbon monoxides ($^{13}C^{16}O$, $^{12}C^{18}O$) and mixtures ($^{12}C^{16}O$ + $^{13}C^{16}O$ and $^{12}C^{16}O$ + $^{12}C^{18}O$) were employed for product identification through isotopic shifts and splittings. The isotopic counterparts are also listed in Table 1.

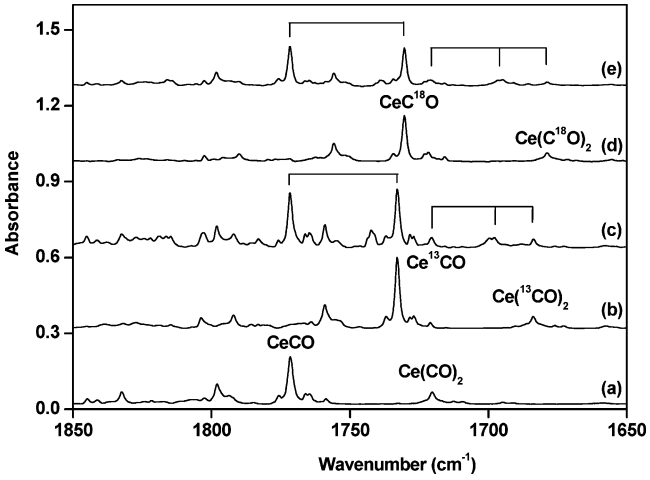

Figure 4. Infrared spectra in the 1850−1650 cm^{-1} region from co-deposition of laser-ablated cerium atoms with isotopic labeled CO in excess argon, taken after 1 h of sample deposition followed by 25 K annealing: (a) 0.1% $^{12}C^{16}O$, (b) 0.1% $^{13}C^{16}O$, (c) 0.05% $^{12}C^{16}O$ + 0.05% $^{13}C^{16}O$, (d) 0.1% $^{12}C^{18}O$, and (e) 0.05% $^{12}C^{16}O$ + 0.05% $^{12}C^{18}O$.

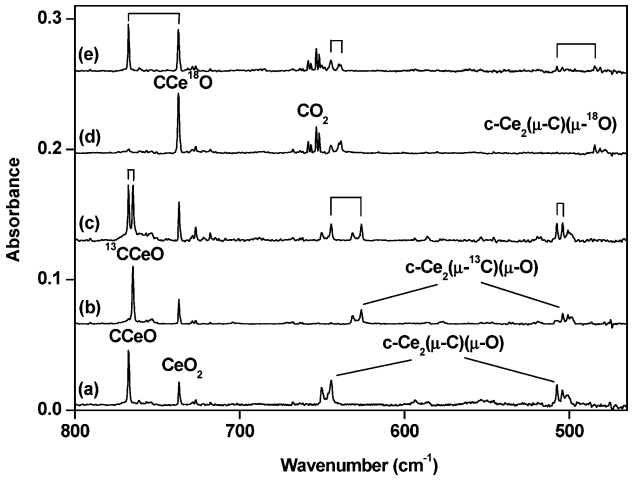

Figure 5. Infrared spectra in the 800−460 cm^{-1} region from co-deposition of laser-ablated cerium atoms with isotopic labeled CO in excess argon, taken after 1 h of sample deposition followed by 25 K annealing: (a) 0.1% $^{12}C^{16}O$, (b) 0.1% $^{13}C^{16}O$, (c) 0.05% $^{12}C^{16}O$ + 0.05% $^{13}C^{16}O$, (d) 0.1% $^{12}C^{18}O$, and (e) 0.05% $^{12}C^{16}O$ + 0.05% $^{12}C^{18}O$.

The spectra in the 1850−1650 and 800−460 cm^{-1} regions using different isotopic CO samples are shown in Figures 4 and 5, respectively.

CeCO. The 1771.8 cm^{-1} band shifted to 1733.0 cm^{-1} with the $^{13}C^{16}O$ sample and to 1730.3 cm^{-1} with the $^{12}C^{18}O$ sample, which yield a $^{12}C/^{13}C$ isotopic frequency ratio of 1.0224 and a $^{16}O/^{18}O$ ratio of 1.0240. In the mixed $^{12}C^{16}O$ + $^{13}C^{16}O$ and $^{12}C^{16}O$ + $^{12}C^{18}O$ experiments, only pure isotopic counterparts were observed, which indicates the formation of a monocarbonyl complex. The 1771.8 cm^{-1} band is therefore assigned to the C−O stretching vibration of the CeCO molecule.

Our B3LYP calculations indicate that the CeCO molecule has a linear structure with a quintet ground state. The predicted Ce−C and C−O bond lengths are 2.289 and 1.172 Å, respectively. The C−O stretching frequency of CeCO was calculated to be 1849.8 cm^{-1}, which is quite close to the experimental frequency, particularly because B3LYP tends to overestimate stretching frequencies in general and the matrix effects are not included in our calculations. The calculated $^{12}C/^{13}C$ and $^{16}O/^{18}O$ isotopic frequency ratio are 1.0227 and 1.0247, respectively, which are in excellent agreement with the experimental values. At the DFT level, the CeCO molecule has a $^5\Delta$ ground state with an electron configuration of (core)$2\delta^1 5\pi^2 11\sigma^1$, which correlates to the $f^1d^2s^1$ excited state of the Ce atom. Both the singly occupied 2δ and 11σ molecular orbitals are quasiatomic nonbonding orbitals, which are largely Ce 4f and 6s in character, respectively. The doubly degenerated 5π MOs comprise extensive Ce 5d to CO $2\pi^*$ back-donation, which accounts for the chemical binding of CO to Ce. Because of this back-donating interaction, the C−O bond is significantly weakened, leading to an elongation of the C−O distance and remarkable reduction of the C−O stretching frequency. The observed 1771.8 cm^{-1} frequency of CeCO is even lower than that of ThCO and is the lowest of any known neutral binary terminal metal carbonyls.[4,14]

CCeO. The 767.4 cm^{-1} band exhibits $^{13}C^{16}O$ and $^{12}C^{18}O$ counterparts at 764.8 and 737.2 cm^{-1}, respectively. The band position and isotopic frequency ratios ($^{12}C/^{13}C$: 1.0034 and $^{16}O/^{18}O$: 1.0410) indicate that this band is largely a terminal Ce−O stretching vibration, but is strongly coupled by carbon atom(s). The isotopic splittings in the mixed $^{12}C^{16}O$ + $^{13}C^{16}O$ and $^{12}C^{16}O$ + $^{12}C^{18}O$ experiments (Figure 5) clearly show that only one C atom and one O atom are involved in this mode. The 767.4 cm^{-1} band was produced upon broad band irradiation during which the CeCO absorption decreased, which suggests that this band is likely due to another isomer of CeCO. Therefore, we assign the 767.4 cm^{-1} band to the Ce−O stretching mode of the inserted CCeO molecule. A very weak band at 646.4 cm^{-1} appeared together with the 767.4 cm^{-1} band. This band shifted to 639.8 cm^{-1} with $^{12}C^{18}O$, but the $^{13}C^{16}O$ counterpart was not observed. This band is tentatively assigned to the Ce−C stretching mode of the CCeO molecule. It is interesting to note that the isotopic $^{16}O/^{18}O$ ratio of the Ce−O stretching mode is much smaller than the diatomic CeO ratio (1.0537), and is even smaller than the ratio of antisymmetric Ce−O stretching mode of CeO_2 (1.0499). Because the Ce−O and Ce−C stretching modes in CCeO are strongly coupled, they are better described as the antisymmetric and symmetric stretching vibrations. To validate the experimental assignment, density functional theory (B3LYP) and ab initio coupled cluster (CCSD(T)) calculations were performed on the CCeO molecule. Geometry optimizations were carried out for the singlet, triplet, and quintet spin states at both levels of theory. The optimized geometric parameters, vibrational frequencies, and isotopic frequency ratios are listed in Table 2. At the B3LYP/basis-I level of theory, a $^5A'$ quintet state with bent structure (Ce−O, 1.831 Å; Ce−C, 2.453 Å; ∠CCeO, 120.2°) was predicted to be the most stable. The lowest triplet state ($^3A'$) with bent structure (Ce−O, 1.805 Å; Ce−C, 2.020 Å; ∠CCeO, 146.2°) is only about 2.1 kcal/mol less stable than the $^5A'$ state. The lowest singlet state ($^1\Sigma$) is linear with Ce−O and Ce−C bond lengths of 1.806 and 1.874 Å. This state lies 4.4 kcal/mol above the $^5A'$ state. The three spin states are too close in energy to be differentiated at the B3LYP level of theory. Indeed, calculations at the CCSD(T)/basis-II level of theory predict the linear singlet state to be the ground state of CCeO, with the bent triplet and quintet states lying 1.7 and 8.2 kcal/mol, respectively, higher in energy than the singlet state.

The calculated vibrational frequencies and isotopic frequency ratios support the assignment of the experimentally observed absorptions to the linear singlet CCeO molecule. As listed in Table 2, the Ce−O and Ce−C stretching modes of CCeO in triplet and quintet states are predicted to be "pure" Ce−O and Ce−C stretching modes without coupling, which are inconsistent with the experimental observations. The two stretching modes

TABLE 2: Calculated Bond Lengths (Å), Bond Angles (deg), Vibrational Frequencies (cm^{-1}), and IR Absorption Intensities (km/mol), and Isotopic Frequency Ratios for Different Spin States of CCeO

		r_{Ce-C}	r_{Ce-O}	∠CCeO	ν_1[a]	ν_2[a]	ν_3[a]	$^{12}C/^{13}C$[b]	$^{16}O/^{18}O$[b]
B3LYP	$^1\Sigma$	1.874	1.806	180.0	808.7	718.7	87.0	1.0086	1.0280
					(301)	(48)	(164)	1.0291	1.0258
	$^3A'$	2.020	1.805	146.2	804.5	598.7	84.9	1.0000	1.0534
					(362)	(46)	(62)	1.0378	1.0008
	$^5A'$	2.453	1.831	120.2	796.1	403.2	117.2	1.0001	1.0540
					(305)	(106)	(26)	1.0370	1.0000
CCSD(T)	$^1\Sigma$	1.882	1.806	180.0	784	667	101		
	$^3A'$	2.042	1.799	120.1	774	400	122		
	$^5A'$	2.453	1.833	116.4	794	405	120		
exp					767.4	646.4		1.0034	1.0410
								−	1.0103

[a] The IR intensities are listed in parentheses. [b] The first number is the ratio for the Ce−O stretching mode (ν_1) and the second number is the ratio for the Ce−C stretching mode (ν_2). The CCSD(T) geometries are optimized with basis-II and the vibrational frequencies are calculated with basis-III (see the text).

TABLE 3: Calculated B3LYP/basis-I Vibrational Frequencies (cm^{-1}) and IR Intensities of the CeCO, $CeCO^-$, $Ce_2[\eta^2(\mu\text{-C,O})]$, and *c*-$Ce_2(\mu\text{-C})(\mu\text{-O})$ Molecules

	frequency (intensity, mode)
CeCO	1849.8 (1276, σ), 337.8 (3, σ), 274.6 (20, π)
$CeCO^-$	1742.3 (1235, σ), 345.8 (1, σ), 271.6 (7, π)
$Ce_2[\eta_2(\mu\text{-C,O})]$	1157.9 (255, a′), 589.9 (5, a′), 466.0 (29, a′), 369.2 (20, a′), 337.9 (20, a″), 115.9 (2, a′)
c-$Ce_2(\mu\text{-C})(\mu\text{-O})$	668.7 (289, b_2), 615.1 (47, a_1), 494.2 (177, a_1), 337.0 (0, b_2), 235.3 (0, a_1), 202.4 (75, b_1)

of the singlet state are computed at 808.7 and 718.7 cm^{-1} and are strongly coupled. The calculated $^{12}C/^{13}C$ and $^{16}O/^{18}O$ isotopic frequency ratios are in reasonable agreement with the experimental values. At the CCSD(T)/basis-III level of theory, the calculated symmetric and asymmetric stretching modes are both in perfect agreement with the observed frequencies, whereas the calculated frequencies of the symmetric modes of the triplet and quintet would be too low to compare with the experiments. The high-level ab initio calculations thus lend further credence to the assignment of a singlet ground state to the CCeO molecule.

$CeCO^-$. Weak absorption at 1694.7 cm^{-1} exhibits isotopic frequency ratios ($^{12}C/^{13}C = 1.0224$ and $^{16}O/^{18}O = 1.0237$) that are characteristic of C−O stretching vibrations of terminal carbonyls. This band is photosensitive, a behavior analogous to most anionic transition-metal carbonyl species in solid argon matrix.[4] No intermediates were observed on both the mixed $^{12}C^{16}O + {}^{13}C^{16}O$ and $^{12}C^{16}O + {}^{12}C^{18}O$ experiments. The 1694.7 cm^{-1} band is thus assigned to the $CeCO^-$ anion, which is predicted to be linear with a quartet ground state (Figure 6). The $^4\Delta$ ground state of $CeCO^-$ is 23.5 kcal/mol lower in energy than the $^5\Delta$ ground state of CeCO at the B3LYP level of theory. The calculated C−O stretching frequency is 1742.3 cm^{-1}, consistent with the experimental measurement.

$Ce_2[\eta^2(\mu\text{-C,O})]$. Weak absorption at 1142.7 cm^{-1} was only observed in the experiments with higher laser energy and relatively low CO concentrations, which implies that the new product involves more than one cerium atom. This band shifts to 1117.7 cm^{-1} with $^{13}C^{16}O$ and to 1122.5 cm^{-1} with $^{12}C^{18}O$. The $^{12}C/^{13}C$ isotopic frequency ratio of 1.0224 and the $^{16}O/^{18}O$ ratio of 1.0180 indicate that this band is due to a C−O stretching vibration. In the mixed $^{12}C^{16}O + {}^{13}C^{16}O$ and $^{12}C^{16}O + {}^{12}C^{18}O$ experiments (Figure 3), only the pure isotopic counterparts were observed, indicating that only one CO subunit is involved in this vibration. The observed C−O stretching frequency of 1142.7 cm^{-1} is unusually low, implying that CO is side-on-bonded. Low C−O stretching frequencies in the range of 1100−1400 cm^{-1} have been reported for some side-on-bonded transition-metal carbonyl clusters and chemisorbed CO on transition-metal surfaces.[25,26] Recently, homoleptic dinuclear group IIIB metal carbonyls with asymmetrically bridging and side-on-bonded CO were characterized to absorb around 1200 cm^{-1} in solid argon.[27]

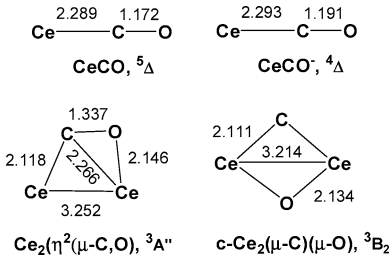

Figure 6. Optimized structures (bond lengths in angstroms, bond angles in degrees) of the CeCO, $CeCO^-$, and two Ce_2CO isomers at the B3LYP/basis-I level of theory.

B3LYP calculations on Ce_2CO predict a rare CO side-on-bonded structure as shown in Figure 6. The molecule has a $^3A''$ ground state with a planar structure. The C atom is bridging bonded to the Ce atoms with two unequivalent Ce−C bonds of 2.118 and 2.266 Å, respectively. The C−O bond length is 1.337 Å, much longer than that of CeCO, and is close to that of the analogous $Sc_2[\eta^2(\mu\text{-C,O})]$ molecule.[27a] The Ce−Ce bond length is predicted to be 3.252 Å and appears to be a weak single bond. The Ce_2 molecule was predicted to have a $^3\Sigma_u^+$ ground state with a bond length of 2.62 Å.[28,29] The C−O stretching frequency for $Ce_2[\eta^2(\mu\text{-C,O})]$ is calculated to be 1157.9 cm^{-1}, just 15.2 cm^{-1} above the observed value. All the other vibrational modes are predicted to have much lower IR intensities than that of the C−O stretching mode and are too weak to be detected.

***c*-$Ce_2(\mu\text{-C})(\mu\text{-O})$.** Absorptions at 644.5 and 507.6 cm^{-1} can be attributed to one species. Each band has one minor site absorption at 650.4 and 504.3 cm^{-1}. The upper band shows a small shift (5.9 cm^{-1}) with $^{12}C^{18}O$ but a large shift (18.2 cm^{-1}) with $^{13}C^{16}O$. On the contrary, the low band shows a large shift (23.0 cm^{-1}) with $^{12}C^{18}O$ but a small shift (3.6 cm^{-1}) with $^{13}C^{16}O$. The mixed $^{12}C^{16}O + {}^{13}C^{16}O$ and $^{12}C^{16}O + {}^{12}C^{18}O$ spectra (Figure 5) clearly show that only one O atom and one C atom are involved in the molecule. The band positions and isotopic frequency shifts suggest the involvement of an unusual cyclic four-membered *c*-$Ce_2(\mu\text{-C})(\mu\text{-O})$ structure.

B3LYP calculations predict the *c*-$Ce_2(\mu\text{-C})(\mu\text{-O})$ molecule to have a planar structure with C_{2v} symmetry (Figure 6). The molecule has a $^3B_2$ ground state with two unpaired 4f electrons occupying the $7b_1$ and $5a_2$ molecular orbitals. The Ce−Ce bond length is computed to be 3.214 Å, very close to that of the $Ce_2[\eta^2(\mu\text{-C,O})]$ complex. The two experimentally observed modes of *c*-$Ce_2(\mu\text{-C})(\mu\text{-O})$ are calculated at 668.7 and 494.2 cm^{-1}, with

289:177 relative intensities. The calculated isotopic frequency ratios (upper mode, $^{12}C/^{13}C = 1.0294$ and $^{16}O/^{18}O = 1.0101$; low mode, $^{12}C/^{13}C = 1.0051$ and $^{16}O/^{18}O = 1.0495$) are also in quite good agreement with the experimental values (upper mode, $^{12}C/^{13}C = 1.0291$ and $^{16}O/^{18}O = 1.0092$; low mode, $^{12}C/^{13}C = 1.0071$ and $^{16}O/^{18}O = 1.0475$) and provide strong support for the experimental assignment of the *c*-$Ce_2(\mu$-C)(μ-O) molecule. Besides the above characterized vibrations, another ring puckering vibration is computed to occur at 615.1 cm^{-1} with IR intensity of 47 km/mol. A weak band at 593.8 cm^{-1} likely arises from this mode.

Other Absorptions. Besides the CeCO absorption, new absorptions at 1720.3, 1832.5, 1845.0, 1925.2, 1953.7, and 1985.1 cm^{-1} are produced on annealing in the terminal C−O stretching frequency region. These absorptions are favored in the experiments with higher CO concentrations. Each absorption exhibits $^{12}C/^{13}C$ and $^{16}O/^{18}O$ isotopic frequency ratios that are characteristic of C−O stretching vibration. These absorptions are due to cerium carbonyls $Ce(CO)_x$ ($x \geq 2$). The 1720.3 cm^{-1} absorption splits into a triplet in the mixed $^{12}C^{16}O + {}^{13}C^{16}O$ and $^{12}C^{16}O + {}^{12}C^{18}O$ experiments and is assigned to $Ce(CO)_2$. The isotopic splittings for the other absorptions cannot be well-resolved because of band overlap; therefore, definitive assignments are difficult. The broad 1985.1 cm^{-1} absorption is the dominant absorption after high-temperature annealing in the experiments with high CO concentration. This band is most likely due to $Ce(CO)_6$. In addition, weak absorptions at 1403.6 and 1386.4 cm^{-1} are produced on annealing in the experiments with relatively higher laser energy. The isotopic shifts also imply that these bands are associated with C−O stretching vibrations. The experimental observations suggest that these bands are from C−O stretching vibrations of side-on-bonded metal cluster carbonyls, indicating that cerium can form a rich family of carbonyl complexes.

Reaction Mechanism. Laser-ablation of cerium metal target produces cerium atoms. Dicerium molecules are also produced during laser ablation or on sample annealing. The cerium carbonyl species are produced upon annealing via the reactions of cerium atoms and dicerium molecules with CO in solid argon, as shown in reactions 1 and 2:

$$Ce + CO \rightarrow CeCO \quad (1)$$

$$Ce_2 + CO \rightarrow Ce_2[\eta^2(\mu\text{-C,O})] \quad (2)$$

The absorptions due to the CCeO and *c*-$Ce_2(\mu$-C)(μ-O) molecules appear on broad-band irradiation, during which the CeCO and $Ce_2[\eta^2(\mu$-C,O)] absorptions are destroyed. It appears that broad-band irradiation initiates the photochemical isomerization reactions 3 and 4:

$$CeCO + h\nu \rightarrow CCeO \quad (3)$$

$$Ce_2[\eta^2(\mu\text{-C,O})] + h\nu \rightarrow c\text{-}Ce_2(\mu\text{-C})(\mu\text{-O}) \quad (4)$$

Theoretical calculations indicate that CeCO has a quintet ground state, whereas the inserted CCeO has a singlet ground state; the monocarbonyl structure is 28.7 kcal/mol more stable than the inserted CCeO isomer at the B3LYP/basis-I level of theory. Therefore, the isomerization reaction 3 is endothermic and involves spin crossing. The reaction proceeds only under $300 < \lambda < 580$ nm irradiation, during which one or more excited states may be involved. The $Ce_2[\eta^2(\mu$-C,O)] carbonyl complex has a very long C−O bond length (1.337 Å). The markedly elongated C−O bond is inclined to dissociation to form the four-membered *c*-$Ce_2(\mu$-C)(μ-O) molecule, which is predicted to be 37.8 kcal/mol more stable than the $Ce_2[\eta^2(\mu$-C,O)] carbonyl isomer. The C−O bond broken process proceeds via a transition state lying 21.6 kcal/mol above the $Ce_2[\eta^2(\mu$-C,O)] complex.

One of the most remarkable aspects of the present experiments is the production of the CCeO and *c*-$Ce_2(\mu$-C)(μ-O) molecules, where CO is activated by the reactions of Ce atoms and Ce_2 molecule with carbon monoxide. CO activation by metal atoms has been observed for some transition-metal, actinide metal, and main-group metal systems.[30−33] The monocarbonyls of Nb, Th, and U can be isomerized to the inserted carbide−oxide molecules on visible light irradiation,[13,14,30] and the dicarbonyls of the Ti and V group metals and actinide metals Th and U undergo photoinduced rearrangement to form C−C bonded isomers.[30,31] However, CO activation by metal diatomics has only been reported for group IIIB metals.[27]

Conclusions

Reactions of Ce atoms and Ce_2 molecules with carbon monoxide molecules in solid argon have been studied using matrix isolation infrared absorption spectroscopy. The cerium monocarbonyl CeCO was produced spontaneously on annealing. The CeCO molecule is calculated to have a $^5\Delta$ ground state with a linear structure, which has the lowest C−O stretching frequency among the known neutral binary metal carbonyls with terminal coordination. Dinuclear metal carbonyl, Ce_2CO, is also produced on annealing at low CO concentrations, which is characterized to have an asymmetrically bridging, side-on-bonded structure. The CeCO and $Ce_2[\eta^2(\mu$-C,O)] carbonyl molecules photochemically rearrange to the CCeO and *c*-$Ce_2(\mu$-C)(μ-O) isomers, where Ce and Ce_2 are inserted into the CO triple bond. The CCeO molecule has a singlet ground state with a linear structure, and the *c*-$Ce_2(\mu$-C)(μ-O) molecule has a triplet ground state with a planar four-membered ring structure. Cerium carbonyl complexes with higher coordination number and $CeCO^-$ anion were also observed.

Acknowledgment. This work is supported by NKBRSF (2004CB719501) and NNSFC (20433080 and 20525104). The calculations were partially performed at the National Laboratory for Information Science and Technology at Tsinghua University.

References and Notes

(1) See, for example: (a) Muetterties, E. L.; Stein, J. *Chem. Rev*. **1979**, *79*, 479. (b) Tatsumi, K.; Nakamura, A.; Hofmann, P.; Stauffert, P.; Hoffmann, R. *J. Am. Chem. Soc*. **1985**, *107*, 4440.

(2) Willner, H.; Aubke, F. *Angew. Chem., Int. Ed. Engl.* **1997**, *36*, 2402.

(3) Lupinetti, A. J.; Strauss, S. H.; Frenking, G. *Prog. Inorg. Chem*. **2001**, *49*, 1.

(4) Zhou, M. F.; Andrews, L.; Bauschlicher, C. W., Jr. *Chem. Rev.* **2001**, *101*, 1931.

(5) Bridgeman, A. J. *Inorg. Chim. Acta*. **2001**, *321*, 27.

(6) Himmel, H. J.; Downs, A. J.; Greene, T. M. *Chem. Rev.* **2002**, *102*, 4191.

(7) Slater, J. L.; Sheline, R. K.; Lin, K. C.; Weltner, W., Jr. *J. Chem. Phys.* **1971**, *55*, 5129.

(8) Slater, J. L.; DeVore, T. C.; Calder, V. *Inorg. Chem.* **1973**, *12*, 1918.

(9) Slater, J. L.; DeVore, T. C.; Calder, V. *Inorg. Chem.* **1974**, *13*, 1808.

(10) Sheline, R. K.; Slater, J. L. *Angew. Chem., Int. Ed. Engl*. **1975**, *14*, 309.

(11) Klotzbucher, W. E.; Petrukhina, M. A.; Sergeev, G. B. *Mendeleev Commun.* **1994**, *1*, 5.

(12) (a) Brennan, J. G.; Andersen, R. A.; Robbins, J. L. *J. Am. Chem. Soc.* **1986**, *108*, 335. (b) Bursten, B. E.; Strittmatter, R. J. *J. Am. Chem. Soc.* **1987**, *109*, 6606. (c) Parry, J.; Carmona, E.; Coles, S.; Hursthouse, M. *J. Am. Chem. Soc.* **1995**, *117*, 2649. (d) Evans, W. J.; Kozimor, S. A.; Nyce, G. W.; Ziller, J. W. *J. Am. Chem. Soc.* **2003**, *125*, 13831.

(13) Zhou, M. F.; Andrews, L.; Li, J.; Bursten, B. E. *J. Am. Chem. Soc*. **1999**, *121*, 9712.

(14) Zhou, M. F.; Andrews, L.; Li, J.; Bursten, B. E. *J. Am. Chem. Soc*. **1999**, *121*, 12188.
(15) (a) Zhou, M. F.; Zhang, L. N.; Dong, J.; Qin, Q. Z. *J. Am. Chem. Soc*. **2000**, *122*, 10680. (b) Wang, G. J.; Chen, M. H.; Zhou, M. F. *J. Phys. Chem. A* **2004**, *108*, 11273.
(16) (a) Becke, A. D. *J. Chem. Phys*. **1993**, *98*, 5648. (b) Lee, C.; Yang, W.; Parr, R. G. *Phys. Rev. B* **1988**, *37*, 785.
(17) (a) McLean, A. D.; Chandler, G. S. *J. Chem. Phys*. **1980**, *72*, 5639. (b) Krishnan, R.; Binkley, J. S.; Seeger, R.; Pople, J. A. *J. Chem. Phys*. **1980**, *72*, 650.
(18) Dolg, M.; Stoll, H.; Preuss, H. *J. Chem. Phys.* **1989**, *90*, 1730.
(19) Gaussian 03, Revision B.05, Frisch, M. J.; Trucks, G. W.; Schlegel, H. B.; Scuseria, G. E.; Robb, M. A.; Cheeseman, J. R.; Montgomery, J. A., Jr.; Vreven, T.; Kudin, K. N.; Burant, J. C.; Millam, J. M.; Iyengar, S. S.; Tomasi, J.; Barone, V.; Mennucci, B.; Cossi, M.; Scalmani, G.; Rega, N.; Petersson, G. A.; Nakatsuji, H.; Hada, M.; Ehara, M.; Toyota, K.; Fukuda, R.; Hasegawa, J.; Ishida, M.; Nakajima, T.; Honda, Y.; Kitao, O.; Nakai, H.; Klene, M.; Li, X.; Knox, J. E.; Hratchian, H. P.; Cross, J. B.; Adamo, C.; Jaramillo, J.; Gomperts, R.; Stratmann, R. E.; Yazyev, O.; Austin, A. J.; Cammi, R.; Pomelli, C.; Ochterski, J. W.; Ayala, P. Y.; Morokuma, K.; Voth, G. A.; Salvador, P.; Dannenberg, J. J.; Zakrzewski, V. G.; Dapprich, S.; Daniels, A. D.; Strain, M. C.; Farkas, O.; Malick, D. K.; Rabuck, A. D.; Raghavachari, K.; Foresman, J. B.; Ortiz, J. V.; Cui, Q.; Baboul, A. G.; Clifford, S.; Cioslowski, J.; Stefanov, B. B.; Liu, G.; Liashenko, A.; Piskorz, P.; Komaromi, I.; Martin, R. L.; Fox, D. J.; Keith, T.; Al-Laham, M. A.; Peng, C. Y.; Nanayakkara, A.; Challacombe, M.; Gill, P. M. W.; Johnson, B.; Chen, W.; Wong, M. W.; Gonzalez, C.; Pople, J. A. Gaussian, Inc.: Pittsburgh, PA, 2003.
(20) Cao, X.; Dolg, M. *J. Chem. Phys.* **2001**, *115*, 7348.
(21) Dunning, T. H., Jr. *J. Chem. Phys.* **1989**, *90*, 1007.
(22) Kendall, R. A.; Dunning, T. H., Jr.; Harrison, R. J. *J. Chem. Phys.* **1992**, *96*, 6796.
(23) MOLPRO is a package of ab initio programs written by Werner, H. J.; Knowles, P. J.; Schütz, M.; Lindh, R.; Celani, P.; Korona, T.; Rauhut, G.; Manby, F. R.; Amos, R. D.; Bernhardsson, A.; Berning, A.; Cooper, D. L.; Deegan, M. J. O.; Dobbyn, A. J.; Eckert, F.; Hampel, C.; Hetzer, G.; Lloyd, A. W.; McNicholas, S. J.; Meyer, W.; Mura, M. E.; Nicklaβ, A.; Palmieri, P.; Pitzer, R.; Schumann, U.; Stoll, H.; Stone, A. J.; Tarroni, R.; Thorsteinsson, T.
(24) Willson, S. P.; Andrews, L. *J. Phys. Chem. A* **1999**, *103*, 3171.
(25) Herrmann, W. A.; Biersack, H.; Ziegler, M. L.; Weidenhammer, K.; Siegel, R.; Rehder, D. *J. Am. Chem. Soc*. **1981**, *103*, 1692.
(26) (a) Hoffmann, F. M.; de Paola, R. A. *Phys. Rev. Lett.* **1984**, *52*, 1697. (b) Shinn, N. D.; Madey, T. E. *Phys. Rev. Lett.* **1984**, *53*, 2481. (c) Moon, D. W.; Bernasek, S. L.; Dwyer, D. J.; Gland, J. L. *J. Am. Chem. Soc.* **1985**, *107*, 4363.
(27) (a) Jiang, L.; Xu, Q. *J. Am. Chem. Soc*. **2005**, *127*, 42. (b) Xu, Q.; Jiang L.; Zou, R. Q. *Chem. Eur.* J. **2006**, *12*, 3226. (c) Jiang L.; Xu, Q. *J. Phys. Chem. A* **2006**, *110*, 5636.
(28) Cao, X. Y.; Dolg, M. *Mol. Phys*. **2003**, *101*, 1967.
(29) Shen, X. L.; Fang, L.; Chen, X. Y.; Lombardi, J. R. *J. Chem. Phys.* **2000**, *113*, 2233.
(30) Zhou, M. F.; Andrews, L. *J. Phys. Chem. A* **1999**, *103*, 7785.
(31) Zhou, M. F.; Andrews, L. *J. Am. Chem. Soc.* **2000**, *122*, 1531.
(32) Zhou, M. F.; Jiang, L.; Xu, Q. *Chem. Eur. J*. **2004**, *10*, 5817.
(33) Zhou, M. F.; Jiang, L.; Xu, Q. *J. Chem. Phys.* **2004**, *121*, 10474.